

## Random lasing action from ZnO–silica nanohybrids

To cite this article: Andreas Stassinopoulos *et al* 2010 *J. Opt.* **12** 024006

View the [article online](#) for updates and enhancements.

### You may also like

- [Random laser emission from dye-doped polymer films enhanced by SiC nanowires](#)  
Yanli Shen, Bingrong Shi, Jian Zhao et al.
- [Red-green-blue plasmonic random lasing from cascaded polymer slices](#)  
Songtao Li, Li Wang, Tianrui Zhai et al.
- [Investigation of the LSPR on a wavelength-tunable random laser](#)  
Zhi Ren, Ning Zheng, Kun Ge et al.

# Random lasing action from ZnO–silica nanohybrids

Andreas Stassinopoulos<sup>1,2</sup>, Rabindra N Das<sup>3</sup>,  
Spiros H Anastasiadis<sup>1,4,5</sup>, Emmanuel P Giannelis<sup>3</sup> and  
Demetrios Anglos<sup>1,4,5</sup>

<sup>1</sup> Institute of Electronic Structure and Laser, Foundation for Research and Technology–Hellas, PO Box 1385, 71110 Heraklion Crete, Greece

<sup>2</sup> Department of Physics, University of Crete, 71103 Heraklion Crete, Greece

<sup>3</sup> Department of Materials Science and Engineering, Cornell University, Ithaca, NY 14853, USA

<sup>4</sup> Department of Chemistry, University of Crete, 71103 Heraklion Crete, Greece

E-mail: [spiros@iesl.forth.gr](mailto:spiros@iesl.forth.gr) and [anglos@iesl.forth.gr](mailto:anglos@iesl.forth.gr)

Received 30 April 2009, accepted for publication 10 June 2009

Published 11 January 2010

Online at [stacks.iop.org/JOpt/12/024006](http://stacks.iop.org/JOpt/12/024006)

## Abstract

Optically active zinc oxide–silica, inorganic–inorganic nanohybrid materials have been synthesized via a sol–gel process utilizing a room temperature scheme that does not require high temperature annealing. Random laser action is demonstrated from these ZnO–silica nanocomposites. The ZnO nanoparticles act as both the gain and the strong scattering medium, which leads to random optical feedback due to multiple elastic scattering, while the amorphous silica matrix offers a high degree of material stability. Optical pumping of the nanocomposites by ultraviolet laser pulses, of duration shorter than the ZnO photoluminescence lifetime, leads to a profound optical gain behavior and random laser action above a certain threshold value of the excitation energy density. In this context, the effects of laser and material parameters on the observed random lasing are investigated for a series of nanocomposites. The observed dependence of the emission wavelength on excitation energy and the excitation energy density value of the random laser threshold are interpreted on the basis of the formation and the inversion of an electron–hole plasma, respectively.

**Keywords:** random lasers, zinc oxide, sol–gel, fluorescent and luminescent materials, nanoscale materials and structures

(Some figures in this article are in colour only in the electronic version)

## 1. Introduction

Following the pioneering theoretical work by Letokhov in the late 1960s [1, 2], experiments by Markushev *et al* on powdered  $\text{Na}_5\text{La}_{1-x}\text{Nd}_x(\text{MoO}_4)_4$  [3] and Lawandy *et al* on solutions containing an organic dye, Rhodamine 640, and  $\text{TiO}_2$  particles [4] demonstrated scattering-assisted optical gain upon laser pumping. This rather unexpected effect was termed random lasing by Lawandy and has generated significant interest in the scientific community. Research has concentrated on understanding the mechanisms driving

the phenomenon, due to its connection to fundamental issues concerning light amplification in disordered media, as well as on the development of materials and structures for novel, effective and low cost light sources. Recent reviews on random lasing detail most of the experimental and theoretical results of the past two decades [5–8], whereas there has been an effort to develop a unified description for lasers and random lasers [9].

Random lasing has been demonstrated with various material structures, including semiconductors [10, 11] and rare earth based materials [12] in powder form, nanocomposite hybrids [13], ceramic materials [14], nanostructured thin films [15–18], semiconducting polymers [19], organic dyes [4, 20–23], liquid crystals [24, 25] and biological

<sup>5</sup> Authors to whom any correspondence should be addressed.

tissues [26, 27]. Potential key advantages of random laser systems include low fabrication cost, ease of production, small size, flexible shape and substrate compatibility and the capability to select the appropriate gain material for a specific lasing frequency. Based on such features, random lasers are expected to find use in various applications such as color coding [11, 28], machine vision [29], sensing of hazardous substances (explosives) [30], search and rescue operations [31], biomedical diagnostics (tumor detection) [26], monitoring the flow of liquids [11], miniature light sources in integrated photonic circuits [11], high brightness displays [32] information technology [33] and more [5–7, 34, 35].

In the context of fabricating and understanding the operation of simple random laser systems, we have investigated various nanocomposite hybrids [13, 16, 21] mostly based on ZnO semiconductor particles which exhibit random laser action upon optical pumping. In such cases, the ZnO particles provide both the gain and the strong scattering power, which leads to light trapping due to multiple elastic scattering and, thus, to random lasing. These ZnO particles can be dispersed in an optically inert polymer matrix [13], which offers ease of material fabrication and processability in view of potential applications, or can be used to fabricate ZnO nanoparticle thin films [16]. In all cases, excitation of the nanohybrids by an ultraviolet laser pulse, with duration shorter than the ZnO photoluminescence lifetime, lead to a pronounced increase of the emitted light intensity, accompanied by a significant spectral and temporal narrowing, when the excitation energy density crosses a certain threshold value.

ZnO is a promising material for photonic applications in the UV spectral range ( $\sim 3.37$  eV bandgap at room temperature, 60 meV exciton binding energy). Thus, there has been great interest in fabricating various ZnO nanostructures and examining their optical properties [36, 37]. Herein, the random laser emission from ZnO–silica based nanocomposites is investigated; these material systems are of considerable interest in nanotechnology for potential applications as varistors, sensor elements, photopiezoelectronics and photoluminescent materials. In general, several preparation methods, like sol-gel [38–43] and impregnation [44–47], have been used for the dispersion of ZnO nanoparticles in silica matrices in order to avoid the tendency of nanoparticles to aggregate. These methods normally require high temperature ( $\sim 600^\circ\text{C}$ ) annealing to obtain photoluminescent active ZnO–silica nanocomposites. In fact, enhanced ultraviolet photoluminescence from sol-gel ZnO–SiO<sub>2</sub> nanocomposites has been reported [38]. The first attempt to show random lasing action from ZnO–silica nanocomposites is described in the study of Leong *et al* [41], who fabricated a thin film of ZnO–SiO<sub>2</sub> on Si, which combined the scattering from the ZnO clusters and the waveguiding of the film in order to achieve laser-like emission. It was not clear whether the feedback mechanism was scattering from the ZnO clusters or waveguiding within the film, since the study examined the light emitted from the edges of the film. The same group fabricated a p-i-n heterostructure junction, in which the intrinsic layer was a ZnO–SiO<sub>2</sub> nanocomposite film [42]; they observed for the first time random lasing action from ZnO–SiO<sub>2</sub> nanocomposites and, even more importantly, random laser action upon electrical pumping. Above a

current threshold of  $\sim 1.5$  mA laser-like emission was observed emerging perpendicular to the film surface.

In the present paper, a new room temperature sol-gel scheme is reported that enables synthesis of ZnO–silica nanocomposites. These inorganic–inorganic nanohybrids consist of commercially available, highly photoluminescent ZnO nanoparticles dispersed in an inert silica matrix synthesized *in situ* from aqueous tetramethoxy silane (TMOS) in the presence of acetic acid. The amorphous silica matrix offers a high degree of material stability while the ZnO nanoparticles act as both the gain medium and centers of strong scattering. Random lasing action is exhibited by these ZnO–silica nanocomposites upon optical pulsed ultraviolet excitation. The effects of material characteristics and irradiation parameters (excitation energy density, pumping volume) on the observed random laser action are presented in this work where the gain mechanism is discussed. In fact, the observed dependence of the emission wavelength on excitation energy and the excitation energy density of the random laser threshold are interpreted on the basis of the formation and the inversion, respectively, of an electron–hole plasma (EHP).

## 2. Experimental details

### 2.1. Specimen preparation

In a typical procedure, ZnO–silica precursor solution was prepared using an appropriate amount of ZnO nanoparticles (Sigma-Aldrich), TMOS and water. The precursor solution was mixed homogeneously in a glass vial and sonicated for 10–30 min. During sonication a catalytic amount of acetic acid (0.1 ml for 1 g TMOS and 1 g water) was added to the precursor solution. Acid addition initiated the gelation process and a semi-solid gel was formed within the sonic bath. The semi-solid gel was kept at room temperature for 24 h to allow completion of the gelation process. This gel was then dried at room temperature for another 24 h and a solid disk shaped ZnO–silica composite was obtained, which was directly used to study the lasing behavior. A series of ZnO–silica composites (20–80 wt% ZnO) were prepared using the present procedure. In terms of macroscopic appearance, the 20 wt% ZnO specimen was quite transparent, whereas as the ZnO concentration reached 33 wt% and more the disks became increasingly milky and totally white above 60 wt% because of multiple scattering.

### 2.2. Specimen characterization

The ZnO–silica nanohybrids were characterized by x-ray diffraction (XRD) and transmission electron microscopy (TEM) and their surface was examined by atomic force microscopy (AFM).

X-ray diffraction studies were performed using a fully automated system (a SCINTAG Inc. theta–theta diffractometer utilizing Cu K $\alpha$  radiation with  $\lambda = 1.54$  Å). An accelerating potential of 45 kV and a current of 40 mA was applied to the copper target. The x-ray diffractograms were recorded with a step size of  $0.02^\circ$  ( $2\theta$ ) and an integration time of 0.24 s per step. Figure 1 shows the XRD patterns of

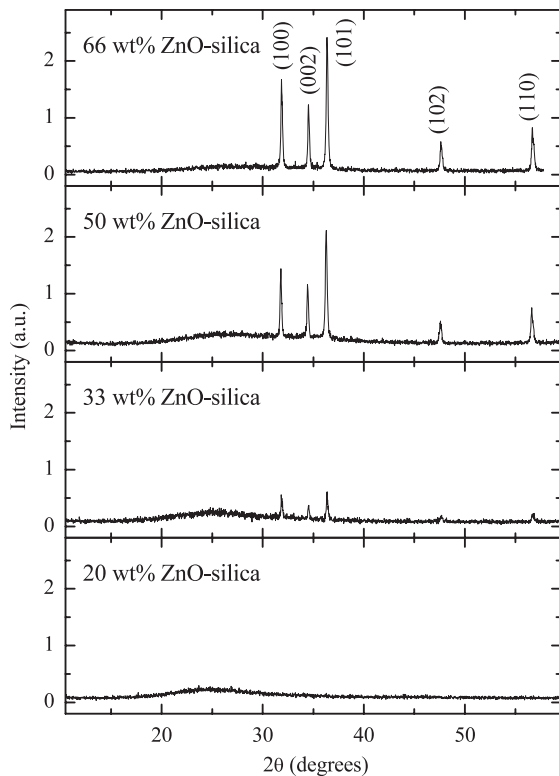


**Figure 1.** X-ray diffractograms from ZnO–silica nanohybrids containing 20, 33, 50 and 66 wt% ZnO (Cu  $K\alpha$  radiation with  $\lambda = 1.54 \text{ \AA}$ ). The assignment of the diffraction peaks corresponds to the ZnO zincite phase (JCPDS card no. 36-1451).

four ZnO–silica nanohybrids. Scattering from crystalline ZnO is observed (Zincite, JCPDS card no. 36-1451) for the 50 and 66 wt% hybrids where the crystallinity increased with increasing concentration of ZnO. However, the 20 wt% ZnO–silica specimen does not exhibit any diffraction peaks associated with crystalline ZnO whereas the 33 wt% hybrid shows extremely weak diffraction peaks. This suggests that the mixing of ZnO with TMOS in the presence of the acid catalyst leads to a chemical reaction that produces an amorphous structure ( $\text{Zn}_2\text{SiO}_4$ ). Thus, in all composites, there should be more than 20 wt% ZnO that reacts with TMOS to produce amorphous structure and the remaining ZnO preserves its crystalline structure. It is noted that amorphous  $\text{Zn}_2\text{SiO}_4$  is widely used as a host [48, 49] for efficient luminescence.

The morphology of the specimens was investigated using a transmission electron microscope (JEOL 1200EX) utilizing thin slices microtomed from the ZnO–silica samples. Figure 2 shows a representative bright field TEM micrograph from the 60 wt% ZnO–silica specimen. Aggregates are observed together with single particles whose average particle size is estimated, based on these TEM images, to be 15–20 nm. Similar ZnO–silica sol–gel TEM images have been observed in the literature [39].

AFM images were recorded in tapping mode (Dimension 3100, Digital Instruments) for the as-prepared ZnO–silica disk specimens in order to examine their surface morphology and roughness. For a typical  $1 \mu\text{m} \times 1 \mu\text{m}$  scan area, the specimen surface appeared to be porous with surface roughness

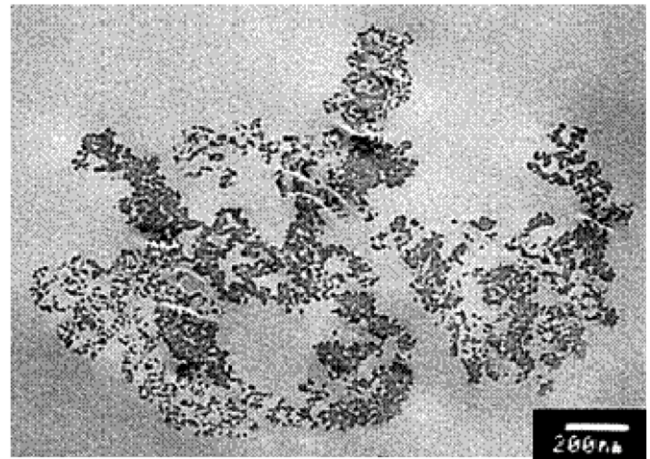


**Figure 2.** Transmission electron microscopy image of a microtomed ZnO–silica nanohybrid containing 60 wt% ZnO. The scale bar corresponds to 200 nm.

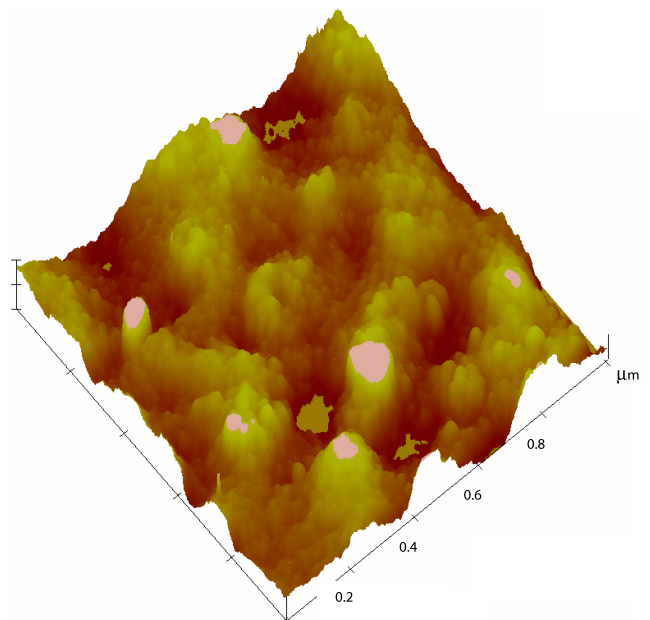


**Figure 3.** Three-dimensional representation of a tapping mode AFM height image ( $1 \mu\text{m} \times 1 \mu\text{m}$ ) of an as-prepared ZnO–silica nanohybrid containing 66 wt% ZnO.  $x, y$ -scale:  $0.2 \mu\text{m}/\text{division}$ .  $z$ -axis scale:  $10 \text{ nm}/\text{division}$ .

of about 25–50 nm. Figure 3 shows a typical AFM image (three-dimensional representation) from the 66 wt% ZnO–silica specimen, where spherical particles with a diameter of about 20–25 nm can be identified, in agreement with the TEM images. The pores observed on the surface were generated upon drying.

### 2.3. Photoluminescence

A 450 fs pulsed KrF excimer-dye laser system (Laser Laboratorium Göttingen) operating at 248 nm was employed as the excitation source [50]. The energy of the laser beam was controlled by means of a variable attenuator in the

range of 0.007–2 mJ/pulse and monitored online through a sensitive energy meter. The irradiation area on the sample surface, typically in the range of 3.5 mm<sup>2</sup>, was adjusted by means of a plano-convex quartz lens ( $f = +500$  mm). The photoluminescence emission was collected through a quartz optical fiber (core diameter 0.6 mm, length 1.5 m) positioned about 15 mm from the sample surface at a 45°-angle with respect to the normal, and introduced into a 0.32 m imaging spectrograph (TRIAx-320, ISA) equipped with a 600 grooves mm<sup>-1</sup> diffraction grating (spectral resolution 0.4 nm, range 80 nm). The spectra were recorded via an intensified charge coupled device (ICCD) detector (DH520, Andor Technology), operated in continuous mode (no gating).

Photoluminescence emission was observed for all the ZnO–silica sol–gel samples with ZnO content greater than 33 wt%. The samples with 20 and 33 wt% of initial ZnO concentration showed no photoluminescence, because most or even all of the ZnO apparently reacted giving Zn<sub>2</sub>SiO<sub>4</sub> as a product. Moreover, the samples with 40, 50 and 55 wt% of initial ZnO concentration showed photoluminescence but no random laser action most probably because of the low concentration of ZnO that remained as particles within the produced specimens. The fact that the 33 wt% ZnO–silica sample shows no photoluminescence emission while the 40 wt% one is photoluminescent suggests that the fraction of ZnO that reacts during the sample preparation procedure must be close to 33 wt%. As a result, it can be assumed that, for example, the sample with 55 wt% of initial concentration of ZnO has an effective ~22 wt% concentration of ZnO. It is noted that at similar and even lower concentrations the same ZnO nanoparticles dispersed within poly(dimethyl siloxane) give rise to strongly scattering composite films and, furthermore, exhibit intense emission and random lasing [13]. In the present paper, the sample composition will be quoted in terms of the nominal amount of ZnO.

### 3. Results and discussion

Figure 4 shows the emission spectra of a ZnO–silica nano hybrid containing 60 wt% ZnO at different levels of excitation energy density (fluence,  $F_{\text{exc}}$ ). The characteristic broadband photoluminescence emission of ZnO is observed at low  $F_{\text{exc}}$ , while random laser action is observed upon strong optical pumping. This is manifested as a significant narrowing of the spectra together with a steep increase of the emission intensity when  $F_{\text{exc}}$  increases above a certain threshold value,  $F_{\text{th}} = 3.4$  mJ cm<sup>-2</sup>. The apparent broadening at very high energy densities ( $F_{\text{exc}} > 7$  mJ cm<sup>-2</sup>) will be further discussed below.

The emission intensity and spectral width are plotted as a function of the excitation energy density for the ZnO–silica specimens with different initial concentration of ZnO (40–75 wt%) and shown in figure 5. Below the threshold energy density,  $F_{\text{th}}$ , the photoluminescence is spectrally broad and characteristic of the nature of the ultraviolet ZnO emission, with a spectral width around 16 nm peaking at 382.4 nm. In this low excitation energy regime the photoluminescence emission intensity varies linearly with  $F_{\text{exc}}$  and the spectral

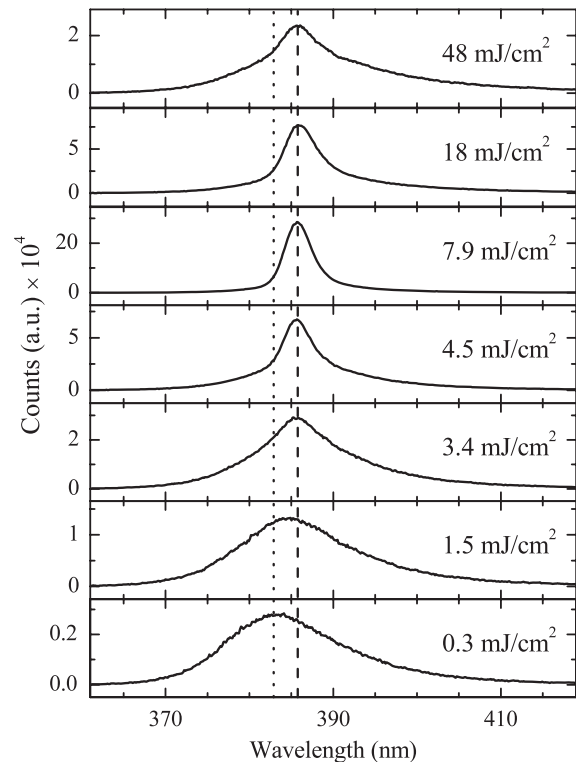


**Figure 4.** Photoluminescence spectra for the ZnO–silica nano hybrid with 60 wt% ZnO for different excitation energy density values (0.3, 1.5, 3.4, 4.5, 7.9, 18 and 48 mJ cm<sup>-2</sup>) upon femtosecond pumping (450 fs, 248 nm) at room temperature. The excitation area is 3.5 mm<sup>2</sup>. The dotted line indicates the peak position for the low excitation energy density (0.3 mJ cm<sup>-2</sup>), whereas the dashed line indicates the peak position for the high excitation energy density (48 mJ cm<sup>-2</sup>)—see the discussion in the text. The excitation energy density threshold value is 3.4 mJ cm<sup>-2</sup> (see text).

width remains constant whereas the peak position of the emission shifts to longer wavelengths (by about 4 nm), or correspondingly to lower energies (figure 6). Actually, the dotted and dashed lines in figure 4 indicate the spectral position of the emission for low and high excitation energy density values, respectively. This profound shift in the peak maximum is attributed to the electron–hole plasma (EHP) [51] known to form under high intensity excitation of ZnO (decay of excitonic effects and transition from exciton to EHP dynamics). Furthermore, above the energy density threshold, there is an obvious gain behavior (figure 5(a)) and a clear spectral narrowing down to 4 nm (figure 5(b)) for all specimens with ZnO content greater than 55 wt%. In parallel, no further redshift of the emission peak is observed (figure 6). The threshold value, for the samples that exhibited random laser action, is around 3.4 mJ cm<sup>-2</sup> and varies slightly for the different ZnO concentrations. Moreover, the threshold energy density for lasing shows a significant increase when the irradiation surface area decreases below 0.4 mm<sup>2</sup> (figure 7), which is in agreement with earlier studies in similar [13, 16] and other systems [14, 52, 53]. This is due to the fact that the decrease of the excitation spot area results in an overall increase of the optical losses leading in turn to an increase of the lasing threshold; it is noted that the optical gain is

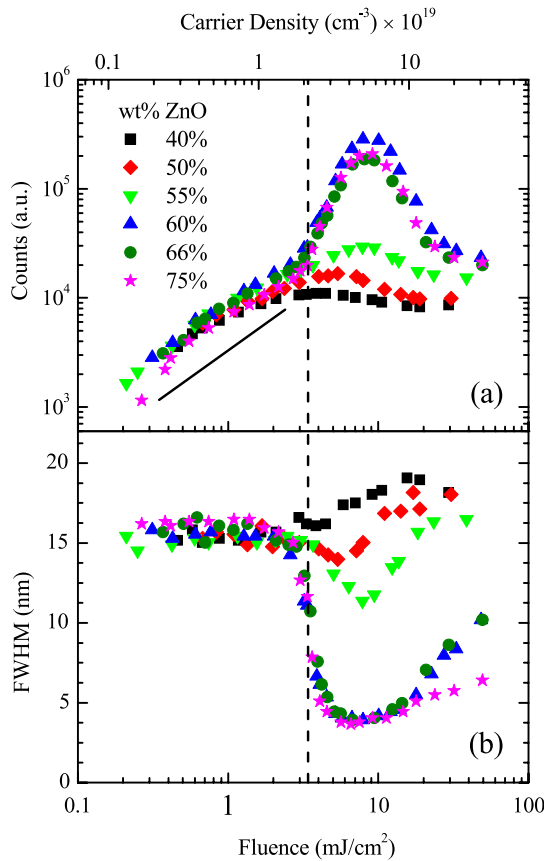


**Figure 5.** (a) Emission intensity and (b) spectral widths (full width at half maximum, FWHM) for a series of ZnO–silica nanocomposites containing 40, 50, 55, 60, 66 and 75 wt% ZnO as a function of the excitation energy density (bottom  $x$ -axis) and the carrier density (top  $x$ -axis). The dashed line indicates the excitation energy density threshold for the 60 wt% ZnO–silica nanocomposite, which is  $3.4 \text{ mJ cm}^{-2}$  ( $\sim 2.1 \times 10^{19} \text{ cm}^{-3}$ ). The solid line indicates a slope equal to 1, indicating the linear dependence observed for energy densities below the threshold. The ZnO–silica nanocomposites are excited with UV femtosecond pulses (450 fs, 248 nm) at room temperature and the excitation area is  $3.5 \text{ mm}^2$ .

proportional to the excitation volume whereas the optical loss is proportional to the total surface area of the gain volume.

It is noted that no laser modes were observed in the present systems. This indicates that the narrow band lasing emission observed under the excitation conditions employed in the present study is due to an incoherent feedback mechanism as opposed to a coherent feedback that could potentially produce sharp spectral features [54].

The origin of the gain mechanism in ZnO can be identified by carefully studying the characteristics of the emission across the fluence range investigated. Optical excitation of ZnO results in the formation of excitons, the density of which is determined by the excitation energy density,  $F_{\text{exc}}$ . At low  $F_{\text{exc}}$  values, free and bound excitons are formed and the photoluminescence emission is the result of excitonic recombination. This is the linear regime for the optical emission processes. Above a critical excitation energy density, excitons begin to interact with each other [55]. At an intermediate  $F_{\text{exc}}$  range, nonlinear optical phenomena emerge

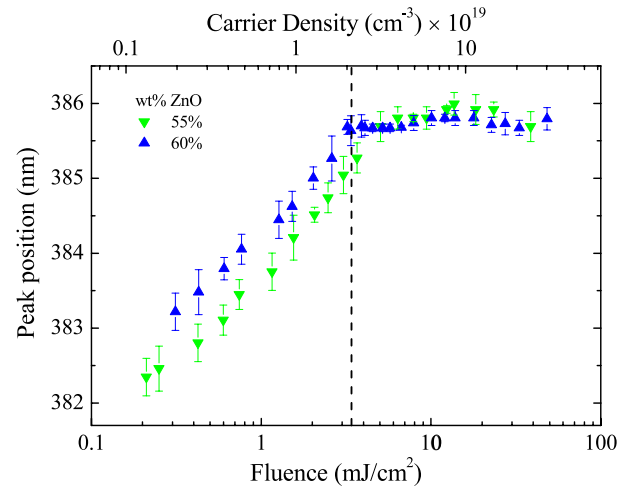


**Figure 6.** The spectral position of the peak intensity for the ZnO–silica nanocomposites containing 55 and 60 wt% ZnO as a function of the excitation energy density upon femtosecond pumping (450 fs, 248 nm) at room temperature. The dashed line indicates the excitation energy density threshold,  $3.4 \text{ mJ cm}^{-2}$  ( $\sim 2.1 \times 10^{19} \text{ cm}^{-3}$ ), for the 60 wt% ZnO–silica specimen. The excitation area is  $3.5 \text{ mm}^2$ .

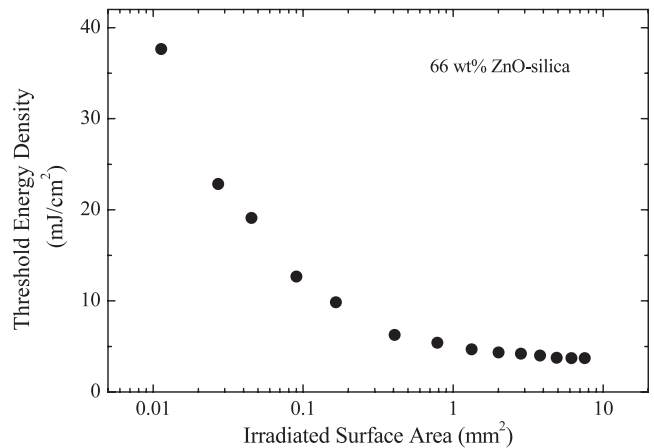


**Figure 7.** Excitation energy density threshold as a function of the irradiated spot area for the 66 wt% ZnO–silica specimen upon femtosecond pumping (450 fs, 248 nm) at room temperature.

as a result of inelastic exciton–exciton scattering. Other known inelastic scattering processes take place between free excitons and free carriers ( $X$ – $e$ ) or LO-phonons ( $X$ – $n\text{LO}$ ) and between bound exciton complexes and free carriers or acoustic phonons [56–62]. In addition, the formation of a new type of carrier, the biexciton (15 meV binding energy [56, 63, 64]), becomes possible at low temperatures. This can be the result of either exciton–exciton collisions [63] or direct resonant two-photon excitation or conversion of an exciton into a biexciton following one-photon absorption [57, 58, 65]. At an even higher  $F_{\text{exc}}$  range, excitons cease to exist as individual quasiparticles because the Coulomb attraction between the electron and the hole is increasingly screened by the large number of neighboring electron–hole pairs resulting in a decrease of the exciton binding energy. When the binding

energy vanishes, a new collective phase of Coulomb-correlated electrons and holes is formed, the so-called electron-hole plasma (EHP) [57, 65], first observed in Si and Ge [66, 67]. The transition from an insulating gas of neutral excitons to the metallic state of an EHP is also known as the Mott transition, occurring at the Mott electron-hole pair density  $n_M$  [55, 68]:

$$n_M^{\text{ZnO}} \approx 0.5 \times 10^{18} \text{ cm}^{-3}. \quad (1)$$

Various parameters, such as sample temperature, feedback mechanism, doping level and others, determine which of the radiative processes discussed above reaches the laser threshold first as excitation energy density increases. Assuming that each absorbed photon creates one electron-hole pair [68], one can write:

$$n_p = \frac{I_{\text{exc}} \tau}{\hbar \omega_{\text{exc}} \ell} \quad (2)$$

where  $n_p$  is the electron-hole pair density ( $\text{cm}^{-3}$ ),  $I_{\text{exc}}$  is the energy flux density ( $\text{W cm}^{-2}$ ) of the excitation beam and  $\hbar \omega_{\text{exc}}$  its photon energy (eV),  $\ell$  is the absorption depth, typically in the range of 1–3  $\mu\text{m}$  [68], whereas the time parameter  $\tau$  is chosen to be the shortest between the laser pulse-width and the ZnO photoluminescence lifetime (275 ps [13]–300 ps [68]).

Based on equations (1) and (2), it is estimated that the EHP is formed at  $F_{\text{exc}} > 0.08 \text{ mJ cm}^{-2}$  (calculated for  $\ell = 2 \mu\text{m}$ ). In the present experiments,  $F_{\text{exc}} > 0.2 \text{ mJ cm}^{-2}$ ; therefore, the carrier density is high enough to create an EHP. It is important to note that the emission peak (e.g. for the 55 wt% ZnO–silica) redshifts (figure 6) from 382.4 nm (3.242 eV) to 386.0 nm (3.212 eV), i.e. by 30 meV. This is in good agreement with the redshift of the EHP emission observed in bulk ZnO [51, 69], which is due to the band gap renormalization (BGR) induced by the increase in carrier density [70–72].

However, this does not automatically imply stimulated emission from the direct recombination of electron-hole pairs in an EHP. This gain process occurs only at an excitation regime in which the EHP is inverted. When the EHP inversion is combined with the appropriate concentration of scattering centers, which provide the basis for a feedback mechanism, random lasing action is triggered. The inversion of the EHP is fulfilled at  $n_p \approx 10^{19} \text{ cm}^{-3}$ , which corresponds to an energy density of about  $1.6 \text{ mJ cm}^{-2}$  [68]. Indeed, the excitation energy density threshold based on the data shown in figure 5 is found to be around  $3.4 \text{ mJ cm}^{-2}$ . This threshold is very similar to that found in earlier studies on ZnO nanocomposite systems for the same excitation area and ZnO nanoparticles [13, 16]. This may suggest that the nature and in turn the optical properties of the particular semiconductor particles are a decisive factor determining the mechanism for lasing, and consequently  $F_{\text{th}}$ . It is noted that totally different systems, such as for example those made by Cao and co-workers, who used electrophoretic or pulsed-laser deposition methods [10, 73], display considerably lower values of  $F_{\text{th}}$ , probably indicating a different gain mechanism.

It is further pointed out that above the excitation energy density, associated with EHP inversion, spectral broadening is observed for those samples that do not exhibit random laser behavior (figure 5(b)). For example, the photoluminescence

corresponding to the 40 wt% ZnO–silica sample has a constant spectral width of 15 nm throughout the intermediate excitation energy density regime while it undergoes a gradual broadening to 19 nm upon entering into the EHP inversion regime ( $F_{\text{exc}} > 3.4 \text{ mJ cm}^{-2}$ ). On the other hand, those samples that exhibit lasing undergo, as expected, a dramatic spectral narrowing above  $F_{\text{th}}$ , reaching spectral widths as short as 4 nm. But notably this narrowing does not persist and, for  $F_{\text{exc}} > 7 \text{ mJ cm}^{-2}$ , the spectra start broadening, their FWHM becoming 6, 10 and 10 nm for the 75, 66 and 60 wt% ZnO–silica samples, respectively. It is worth noting that in the case of the 50 and 55 wt% ZnO–silica samples a limited narrowing is observed when crossing into the EHP inversion regime, which is, however, totally reversed as excitation energy density is increased further. This spectral broadening behavior, observed in all samples, is actually correlated with the broadening of the gain spectrum, known to be a result of electron-hole plasma formation [55, 68, 70, 74]. In fact, this effect may be what inhibits the 50 and 55 wt% ZnO–silica samples from lasing.

Parallel to the spectral broadening behavior, discussed above, it is observed that for  $F_{\text{exc}} > 7 \text{ mJ cm}^{-2}$  the emission intensity drops significantly. Similar behavior has been observed with ZnO nanorods that exhibit a decrease in the stimulated emission intensity above a certain value of excitation power [75]; that was attributed to heating or damage of the material. However, no damage was observed in the specimens studied, even for excitation energy densities as high as  $50 \text{ mJ cm}^{-2}$ . In fact, the emission intensity dependence on excitation energy density (figure 5(a)) is fully reversible when going from low to high and back to low fluence values.

Finally, in figure 5(a), it can be seen that, as the concentration increases from 60 to 75 wt% ZnO, the emission intensity slightly decreases (and even more for the 80 wt% ZnO–silica sample) for the same value of excitation energy density even below the random lasing threshold. This could be attributed to higher surface scattering with increasing ZnO concentration [16] that prevents the efficient coupling of the pumping light into the gain material.

## 4. Conclusions

ZnO–silica based nanocomposites were synthesized via a sol-gel process utilizing a room temperature scheme that does not require high temperature annealing in order to obtain the optically active inorganic–inorganic nanohybrids. The random lasing behavior has been investigated for these hybrid materials. Upon excitation with a short-pulse UV laser, a profound optical gain behavior was observed above a certain threshold value of the pump energy density.

Moreover, the gain mechanism and the excitation energy density threshold value for the random laser emission from a series of ZnO–silica nanohybrids investigated have been explained on the basis of formation and inversion of the electron-hole plasma (EHP), respectively. In order to trigger the random laser action upon EHP inversion, it is necessary to have a high concentration of strongly scattering particles, which provide the basis for the feedback mechanism.

The absence of a high temperature annealing processing step would allow the *in situ* integration of such hybrids even on plastic flexible substrates, which could potentially contribute to the easier development of electrical pumped random laser sources [42, 76, 77].

## Acknowledgments

The authors would like to thank A Englezis for technical support with the femtosecond laser. This work was supported in part by the General Secretariat for Research and Technology, Greece (project ΠΕΝΕΔ, contract 03ΕΔ581), by the European Office for Aerospace Research and Development, EOARD, under contract SPC 01-4070, and by the Ultraviolet Laser Facility operating at IESL-FORTH supported through the access activities of the EC FP6 project 'Laserlab-Europe' RII3-CT-2003-506350.

## References

- [1] Letokhov V S 1967 *JETP Lett.* **5** 212
- [2] Letokhov V S 1968 *Sov. Phys.—JETP* **26** 835
- [3] Markushev V M, Zolin V F and Briskina C M 1986 *Sov. J. Quantum Electron.* **16** 281
- [4] Lawandy N M, Balachandran R M, Gomes A S L and Sauvain E 1994 *Nature* **368** 436
- [5] Noginov M A and Letokhov V S 2005 *Solid-State Random Lasers* (New York: Springer)
- [6] Wiersma D S 2008 *Nat. Phys.* **4** 359
- [7] Cao H 2003 *Waves Random Media* **13** R1
- [8] Cao H 2005 *J. Phys. A: Math. Gen.* **38** 10497
- [9] Türeci H E, Ge L, Rotter S and Stone A D 2008 *Science* **320** 643
- [10] Cao H, Zhao Y G, Ho S T, Seelig E W, Wang Q H and Chang R P H 1999 *Phys. Rev. Lett.* **82** 2278
- [11] Wiersma D S 2000 *Nature* **406** 132
- [12] Noginov M A, Zhu G, Frantz A A, Novak J, Williams S N and Fowlkes I 2004 *J. Opt. Soc. Am. B* **21** 191
- [13] Anglos D, Stassinopoulos A, Das R N, Zacharakis G, Psyllaki M, Jakubiak R, Vaia R A, Giannelis E P and Anastasiadis S H 2004 *J. Opt. Soc. Am. B* **21** 208
- [14] Bahoura M, Morris K J and Noginov M A 2002 *Opt. Commun.* **201** 405
- [15] Huang M H, Mao S, Feick H, Yan H Q, Wu Y Y, Kind H, Weber E, Russo R and Yang P D 2001 *Science* **292** 1897
- [16] Stassinopoulos A, Das R N, Giannelis E P, Anastasiadis S H and Anglos D 2005 *Appl. Surf. Sci.* **247** 18
- [17] Lau S P, Yang H Y, Yu S F, Yuen C, Leong E S P, Li H D and Hng H H 2005 *Small* **1** 956
- [18] Ursaki V V, Burlacu A, Rusu E V, Postolake V and Tiginyanu I M 2009 *J. Opt. A: Pure Appl. Opt.* **11** 075001
- [19] Hide F, Schwartz B J, Díaz-García M A and Heeger A J 1996 *Chem. Phys. Lett.* **256** 424
- [20] Zacharakis G, Papadogiannis N A and Papazoglou T G 2002 *Appl. Phys. Lett.* **81** 2511
- [21] Papadakis V M, Stassinopoulos A, Anglos D, Anastasiadis S H, Giannelis E P and Papazoglou D G 2007 *J. Opt. Soc. Am. B* **24** 31
- [22] de Matos C J S, Menezes L D S, Brito-Silva A M, Gámez M A M, Gomes A S L and de Araújo C B 2007 *Phys. Rev. Lett.* **99** 153903
- [23] Zhang D K, Chen Z Y and Ma D 2008 *J. Appl. Phys.* **103** 123103
- [24] Wiersma D S and Cavalieri S 2001 *Nature* **414** 708
- [25] Ferjani S, Barna V, De Luca A, Versace C and Strangi G 2008 *Opt. Lett.* **33** 557
- [26] Polson R C and Vardeny Z V 2004 *Appl. Phys. Lett.* **85** 1289
- [27] Siddique M, Yang L, Wang Q Z and Alfano R R 1995 *Opt. Commun.* **117** 475
- [28] Ramachandran H 2002 *Pramana J. Phys.* **58** 313
- [29] Lawandy N M 1994 *Photon Spectra.* **28** 119
- [30] Rose A, Zhu Z G, Madigan C F, Swager T M and Bulović V 2005 *Nature* **434** 876
- [31] Field C T and Millar P S 1999 *Appl. Opt.* **38** 2586
- [32] Williams G, Rand S C, Hinklin T and Laine R M 1999 *Conf. Laser and Electro-Optics, OSA Technical Digest* (Washington, DC: Optical Society of America) p 90
- [33] Lichmanov A A, Briskina C M, Soshchin N P and Zolin V F 1999 *Bull. Russ. Acad. Sci.* **63** 922
- [34] Rand S C 2003 *Opt. Photon. News* **14** 32
- [35] Cao H 2005 *Opt. Photon. News* **16** 24
- [36] Özgür Ü, Alivov Y I, Liu C, Teke A, Reshchikov M A, Doğan S, Avrutin V, Cho S J and Morkoç H 2005 *J. Appl. Phys.* **98** 041301
- [37] Djurišić A B and Leung Y H 2006 *Small* **2** 944
- [38] Fu Z P, Yang B F, Li L, Dong W W, Jia C and Wu W 2003 *J. Phys.: Condens. Matter* **15** 2867
- [39] Cannas C, Casu M, Lai A, Musinu A and Piccaluga G 1999 *J. Mater. Chem.* **9** 1765
- [40] Lorenz C, Emmerling A, Fricke J, Schmidt T, Hilgendorff M, Spanhel L and Müller G 1998 *J. Non-Cryst. Solids* **238** 1
- [41] Leong E S P, Chong M K, Yu S F and Pita K 2004 *IEEE Photon. Technol. Lett.* **16** 2418
- [42] Leong E S P and Yu S F 2006 *Adv. Mater.* **18** 1685
- [43] Musat V, Fortunato E, Petrescu S and Botelho do Rego A M 2008 *Phys. Status Solidi a* **205** 2075
- [44] Zhang W H, Shi J L, Wang L Z and Yan D S 2000 *Chem. Mater.* **12** 1408
- [45] Yao B D, Shi H Z, Bi H J and Zhang L D 2000 *J. Phys.: Condens. Matter* **12** 6265
- [46] Khouchaf L, Tuillier M H, Wark M, Paillaud J J and Souillard M 1997 *J. Physique IV* **7** 267
- [47] Cannas C, Mainas M, Musinu A and Piccaluga G 2003 *Compos. Sci. Technol.* **63** 1187
- [48] Morimo R and Matae K 1989 *Mater. Res. Bull.* **24** 175
- [49] Su K, Tilley T D and Sailor M J 1996 *J. Am. Chem. Soc.* **118** 3459
- [50] Szatmári S and Schäfer F P 1988 *Opt. Commun.* **68** 196
- [51] Klingshirn C 1992 *J. Cryst. Growth* **117** 753
- [52] van Soest G, Tomita M and Legendijk A 1999 *Opt. Lett.* **24** 306
- [53] Ling Y, Cao H, Burin A L, Ratner M A, Liu C and Chang R P H 2001 *Phys. Rev. A* **64** 063808
- [54] Cao H, Xu J Y, Chang S H and Ho S T 2000 *Phys. Rev. E* **61** 1985
- [55] Klingshirn C 2007 *ChemPhysChem* **8** 782
- [56] Klingshirn C et al 2006 *Excitonic Properties of ZnO* (Berlin: Springer)
- [57] Klingshirn C and Haug H 1981 *Phys. Rep.* **70** 315
- [58] Klingshirn C F 2007 *Semiconductor Optics* (Berlin: Springer)
- [59] Klingshirn C 1975 *Phys. Status Solidi b* **71** 547
- [60] Hvam J M 1973 *Solid State Commun.* **12** 95
- [61] Hvam J M 1974 *Phys. Status Solidi b* **63** 511
- [62] Koch S W, Haug H, Schmieder G, Bohnert W and Klingshirn C 1978 *Phys. Status Solidi b* **89** 431
- [63] Hvam J M, Blattner G, Reuscher M and Klingshirn C 1983 *Phys. Status Solidi b* **118** 179
- [64] Klingshirn C, Hauschild R, Priller H, Decker M, Zeller J and Kalt H 2005 *Superlatt. Microstruct.* **38** 209
- [65] Hönerlage B, Lévy R, Grun J B, Klingshirn C and Bohnert K 1985 *Phys. Rep.* **124** 161
- [66] Rice T M 1977 *Electron-Hole Liquids in Semiconductors I: Theory (Solid State Physics vol 32)* ed F S H Ehrenreich and D Turnbull (New York: Academic Press) p 1
- [67] Hensel J C, Phillips T G and Thomas G A 1977 *The Electron-Hole Liquid in Semiconductors: Experimental Aspects (Solid State Physics vol 32)* ed F S H Ehrenreich and D Turnbull (New York: Academic Press) p 87

- [68] Klingshirn C, Hauschild R, Fallert J and Kalt H 2007 *Phys. Rev. B* **75** 115203
- [69] Tang Z K, Wong G K L, Yu P, Kawasaki M, Ohtomo A, Koinuma H and Segawa Y 1998 *Appl. Phys. Lett.* **72** 3270
- [70] Priller H, Brückner J, Gruber T, Klingshirn G, Kalt H, Waag S X, Ko H J and Yao T 2004 *Phys. Status Solidi b* **241** 587
- [71] Bohnert K, Schmieder G and Klingshirn C 1980 *Phys. Status Solidi b* **98** 175
- [72] Bohnert K, Anselment M, Kobbe G, Klingshirn C, Haug H, Koch S W, Schmittrink S and Abraham F F 1981 *Z. Phys. B* **42** 1
- [73] Cao H, Zhao Y G, Ong H C, Ho S T, Dai J Y, Wu J Y and Chang R P H 1998 *Appl. Phys. Lett.* **73** 3656
- [74] Müller G O, Rösler M, Weber H H and Zimmermann R 1976 High excitation of direct semiconductors like CdS *Physics of Highly Excited States in Solids: Proceedings of the 1975 Oji Seminar (Tomakomai, Sept., 1975) (Lecture Notes in Physics vol 57)* (Berlin, New York: Springer-Verlag) p 349
- [75] Fallert J, Stelzl F, Zhou H, Reiser A, Thonke K, Sauer R, Klingshirn C and Kalt H 2008 *Opt. Express* **16** 1125
- [76] Ma X Y, Chen P L, Li D S, Zhang Y Y and Yang D R 2007 *Appl. Phys. Lett.* **91** 251109
- [77] Chen P, Ma X, Li D, Zhang Y and Yang D 2009 *Opt. Express* **17** 4712